Measuring prions by bioluminescence imaging

Gültekin Tamgüney[a,b], Kevin P. Francis[c], Kurt Giles[a,b], Azucena Lemus[d], Stephen J. DeArmond[a,d], and Stanley B. Prusiner[a,b,1]

[a]Institute for Neurodegenerative Diseases and Departments of [b]Neurology and [d]Pathology, University of California, San Francisco, CA 94143; and [c]Caliper Life Sciences, Alameda, CA 94501

Contributed by Stanley B. Prusiner, July 1, 2009 (sent for review May 28, 2009)

Prions are infectious proteins that cause fatal neurodegenerative diseases. Because astrocytic gliosis marked by the deposition of fibrils composed of GFAP is a prominent feature of prion disease, we asked whether GFAP might be used as a surrogate marker for prions. To interrogate this posit, we inoculated prions into transgenic (Tg) mice expressing luciferase (luc) under the GFAP gene (*Gfap*) promoter, denoted Tg(*Gfap*-luc) mice. Weekly noninvasive, bioluminescence imaging (BLI) detected an increase in light emitted from the brains of Tg(*Gfap*-luc) mice at ≈55 d after inoculation and ≈62 d before neurologic deficits appeared. To determine whether BLI could be used as a proxy bioassay for prion infectivity, we performed endpoint titrations of prions in Tg(*Gfap*-luc) mice. BLI bioassays were as or more sensitive than those determined by the onset of neurological dysfunction, and were completed in approximately half the time. Our studies argue that BLI is likely to be a suitable surrogate for measuring prion infectivity, and might be useful in the study of Tg mouse models for other neurodegenerative illnesses.

astrocytic gliosis | bioassay | GFAP | neurodegeneration

Prions cause neurodegenerative diseases of humans and animals (1–5). The discovery of PrP^{Sc}, the sole component of the infectious prion, revolutionized studies of the prion diseases (6–8). Before the identification of PrP^{Sc}, all measurements of prions required bioassays in experimental animals (9, 10). Kinetic studies showed that PrP^{Sc} could be detected in brain by immunoassay long before signs of neurological dysfunction appeared. However, such immunoassays required sacrifice of experimental animals and removal of the brain (11).

With the development of incubation-time assays for prions, purification and characterization of scrapie infectivity were able to proceed (12, 13). In such assays, the interval from inoculation to the onset of clinical signs is inversely related to the dose of prions injected intracerebrally (i.c.) (10). Over the past three decades, improvements in measuring prion infectivity have been limited to using transgenic (Tg) mice that overexpress PrP^{C}, which often leads to a reduction in the incubation time (14–16), and to using cultured mouse neuroblastoma (N2a) cells (17, 18). Unfortunately, only a few strains of mouse prions can be used to infect cultured N2a cells (19), and the efficiency of infection is frequently low (17).

We report here on the use of bioluminescence imaging (BLI) to measure prions in the brains of mice. We began by asking whether prion replication would induce a detectable luminescence in the brains of Tg(*Gfap*-luc) mice (luc, luciferase). Earlier studies had shown that prions stimulate astrocytes to express GFAP, which assembles into fibrils (20–23), but is not required for prion disease pathogenesis (24). After i.c. inoculation of prions, we imaged the mice weekly to establish the background level of BL in both control and prion-infected Tg(*Gfap*-luc) mice. At ≈55 d postinoculation (pi), an inflection in the luminescence curve was detected in the prion-infected, but not the control Tg(*Gfap*-luc) mice. Over the next 21 d, the level of luminescence increased progressively until it reached a plateau and remained elevated until the animals developed signs of neurological dysfunction ≈62 d later. To determine whether BLI could be used as a proxy bioassay for prion infectivity, we performed endpoint titrations of prions in Tg(*Gfap*-luc) mice by inoculating serial 10-fold dilutions of a brain homogenate. Bioassays using BLI were as or more sensitive than those determined by the onset of neurological dysfunction, and were completed in approximately half the time. While our studies were in progress, an article was published that reported increased BL in asymptomatic [Tg(*Gfap*-luc/SOD1,G93A)] mice, a model for amyotrophic lateral sclerosis (25); those findings as well as the data reported here demonstrate the potential applicability of BLI for other neurodegenerative disorders.

Results

Using an IVIS Spectrum imaging system, we quantified the BL emitted from the brains of Tg(*Gfap*-luc) mice (Fig. 1*A*) at various time points (dpi). BL was significantly elevated in prion-infected brains at 55 dpi (Fig. 1*C*) compared with controls at 56 dpi ($P < 0.005$, Bonferroni *t* test) (Fig. 1*D*) and to the same prion-infected mice at 48 dpi ($P < 0.001$, Bonferroni *t* test) (Fig. 1*B*). No difference in BL was found ($P > 0.5$, Bonferroni *t* test) between prion-infected mice at 48 dpi (Fig. 1*B*) and control mice at 56 dpi (Fig. 1*D*). Based on these results, we chose BL values $\geq 2 \times 10^6$ photons/s as indicative of luc expression induced by prion replication. In prion-infected mice, the median time for an increase in *Gfap*-luc transgene expression was 55 ± 2.8 dpi (Fig. 1*E*). Signs of neurological dysfunction in the same mice were apparent ≈62 d later, yielding a median incubation time of 117 ± 1.1 dpi (Fig. 1*E*). Control mice neither showed increased *Gfap*-luc expression nor developed neurological dysfunction throughout the course of the experiment.

We also inoculated groups of 12 Tg(*Gfap*-luc) mice with RML prions either i.p. or by oral gavage. Mice inoculated i.p. showed increased CNS BL after a median incubation time of 129 ± 12.4 dpi and died after a median incubation time of 167 ± 22.3 dpi. Mice inoculated by oral gavage exhibited elevated CNS BL after a median incubation time of 154 ± 9.4 dpi and died after a median incubation time of 216.5 ± 5.7 dpi (Fig. S1). For these routes of infection, increased BL preceded clinical signs by ≈40–60 d, despite longer incubation periods compared with i.c. inoculation.

To determine the kinetics of prion accumulation, reactive astrocytic gliosis, and BL in prion-inoculated Tg(*Gfap*-luc) mice, we measured PrP^{Sc}, GFAP mRNA, and BL between 21 and 61 dpi. PrP 27-30, the proteinase K-resistant fragment of PrP^{Sc}, was detected in the brains of infected mice beginning at 42 dpi and progressively increased thereafter (Fig. 2*A*). Immunohistochemistry for PrP also showed PrP^{Sc} deposits in brain tissue taken at 42 dpi (Fig. 3). GFAP mRNA levels as measured by qRT-PCR were elevated at 56 dpi, at which time the BL had also increased

Author contributions: G.T. and S.B.P. designed research; G.T., K.P.F., A.L., and S.J.D. performed research; K.G. contributed new reagents/analytic tools; G.T., S.J.D., and S.B.P. analyzed data; and G.T., S.J.D., and S.B.P. wrote the paper.

The authors declare no conflict of interest.

[1]To whom correspondence should be addressed. E-mail: stanley@ind.ucsf.edu.

This article contains supporting information online at www.pnas.org/cgi/content/full/0907339106/DCSupplemental.

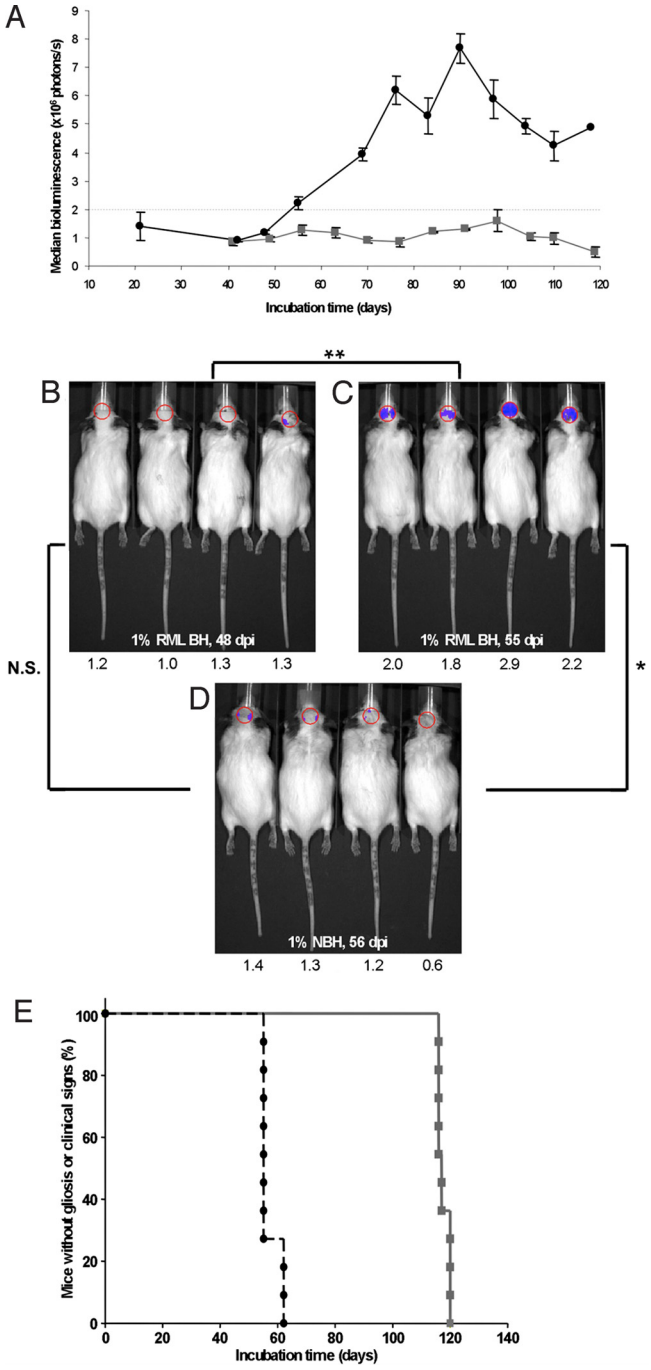

Fig. 1. BL in Tg(*Gfap*-luc) mice i.c. inoculated with RML prions ($n = 12$) indicates reactive astrocytic gliosis. (*A*) BL measured from the brains of prion-inoculated mice (black circles) begins to increase at 55 dpi. BL in control Tg(*Gfap*-luc) mice inoculated with 1% normal brain homogenate (NBH) ($n = 4$, gray squares) remains low throughout the incubation period. (*B–D*) Photos of representative Tg(*Gfap*-luc) mice, with overlays of the circular area above the brain from which BL was quantified. The BL measured, $\times 10^6$ photons/s, from each mouse brain is shown below each image. The BL measured from the brains of prion-infected mice significantly increased (**, $P < 0.001$, Bonferroni *t* test) from 48 dpi (*B*) to 55 dpi (*C*). Similarly, BL measured from infected mice at 55 dpi (*C*) was also significantly (*, $P < 0.005$) greater than in control mice inoculated with NBH and imaged at 56 dpi (*D*). No significant difference (N.S., $P > 0.5$) was measured between RML-inoculated mice at 48 dpi (*B*) and control mice at 56 dpi (*D*). Based on this result, we determined that astrocytic gliosis was detectable at BL values $\geq 2.0 \times 10^6$ photons/s. (*E*) Kaplan–Meier plots for incubation times based on the appearance clinical signs (gray squares) or on the onset of reactive astrocytic gliosis (black circles). The median onset time for clinical signs was 117 ± 1.1 dpi (95% confidence interval), whereas that for gliosis was 55 ± 2.8 dpi.

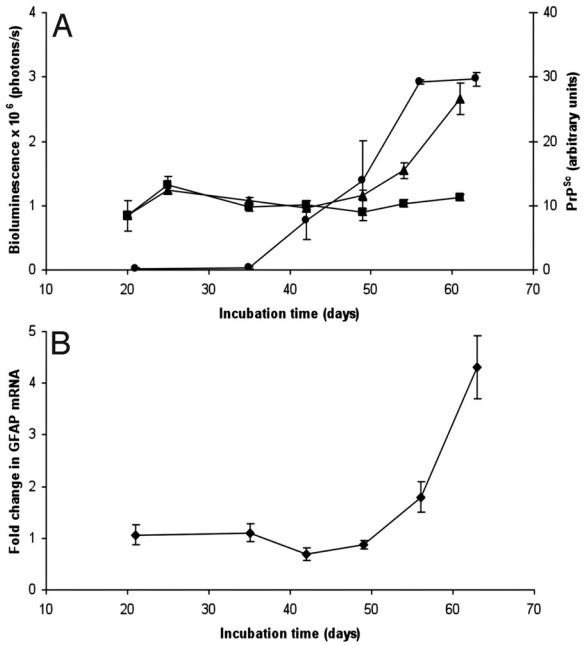

Fig. 2. During prion infection, increases in PrP^{Sc} preceded increases in BL (*A*) and GFAP mRNA (*B*). (*A*) Protease-resistant PrP^{Sc} (circles, right ordinate) in the brains of RML-infected Tg(*Gfap*-luc) mice began to accumulate at 42 dpi and increased steadily. PrP^{Sc} levels were quantified at each time point by densitometry of Western blottings. BL (triangles, left ordinate) in the brains of infected Tg(*Gfap*-luc) mice increased beginning at 56 dpi, ≈14 d after PrP^{Sc} accumulation. BL measured from the brains of control mice inoculated with 1% NBH did not increase (squares). (*B*) Correlating with an increase of BL, GFAP mRNA also increased at ≈56 dpi. Error bars indicate the SE, based on at least 9 mice for BL measurements and 3 mice for all other measurements.

(Fig. 2*B*). Immunohistochemistry for GFAP showed reactive astrocytic gliosis in the brain beginning at 49 dpi (Fig. 3). Control Tg(*Gfap*-luc) mice did not show PrP^{Sc} in their brains as detected by immunohistochemistry (Fig. 3) or increased GFAP levels as monitored by qRT-PCR, immunohistochemistry, and BL.

Convinced that BLI could be used as a surrogate for prion infection, we asked whether the interval from inoculation to the point of inflection in BL could be used to measure the prion titer in the inoculum. To investigate this possibility, we inoculated nine additional groups of 12 mice with serial 10-fold dilutions, ranging from 10^{-2} to 10^{-10}, of a 10% (wt/vol) Rocky Mountain Laboratory (RML) brain homogenate. All mice were imaged weekly until they developed clinical signs or the experiment was terminated (Fig. 4*A*; Fig. S2). We observed an inverse correlation between the inoculated dose and the interval from inoculation to the BL point of inflection, corresponding to $\geq 2 \times 10^6$ photons/s. Using the method of Spearman–Kärber (26), we calculated a prion titer of 8.3 ± 0.3 log ID_{50} units/mL based on the appearance of neurological signs, and a titer 9.3 ± 0.3 log ID_{50} units/mL as determined by BLI. The difference in these calculated titers is due to fewer censored animals and a greater number of preclinical cases in the BLI dataset (Table S1). In some prion-infected mice that died without developing overt neurological deficits, reactive astrocytic gliosis was detected by BLI. In other mice inoculated with high dilutions, some were positive by BLI, but failed to develop clinical signs of neurological dysfunction throughout the course of the experiment. Based on the calculated titer, we plotted the dose of prions in the inoculum as a function of the median incubation times for appearance of clinical signs (gray curve in Fig. 4*B*) or for astrocytic gliosis based on BLI (black curve in Fig. 4*B*). Also, we found a linear correlation between the median incubation times

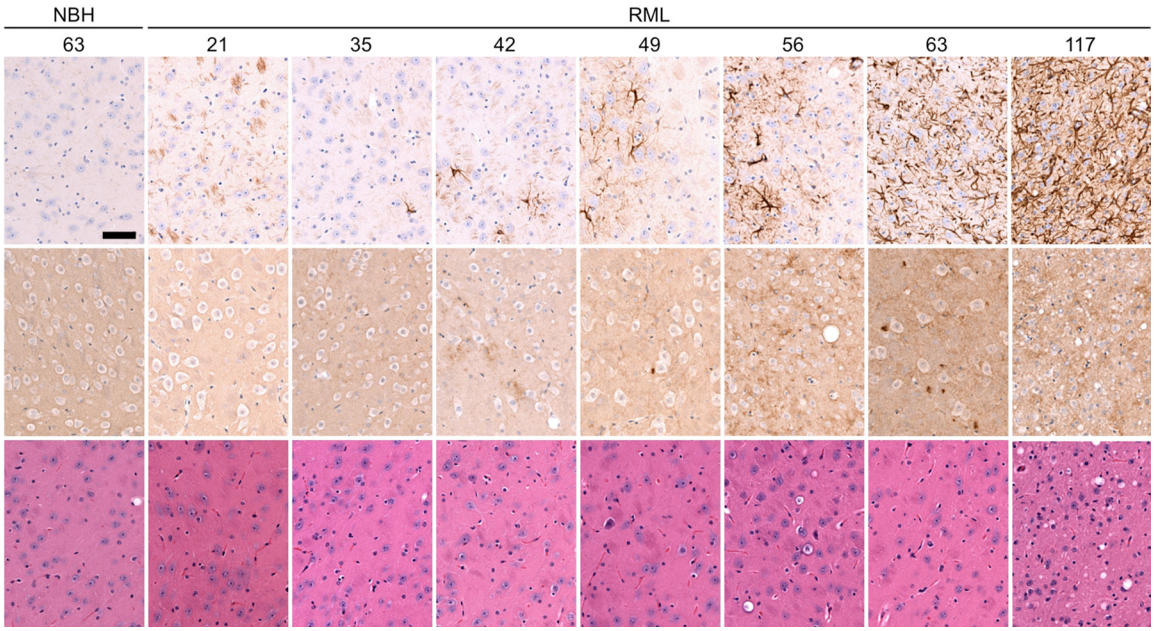

Fig. 3. Immunohistochemistry of thalamic brain sections from Tg(*Gfap*-luc) mice show time-dependent progression of reactive astrocytic gliosis and neuropathology after RML inoculation. Tg(*Gfap*-luc) mice inoculated with 1% NBH are shown as controls. Mice were killed at the time (dpi) indicated above each column. Sections were stained with peroxidase for GFAP (*Top*), anti-PrP antibodies for PrP^{Sc} deposition (*Middle*), and hematoxylin and eosin for vacuolation (*Bottom*). At 21 dpi, both RML-inoculated and control mice developed some mild gliosis due to inoculation-induced trauma that disappeared at 35 dpi. In contrast to control mice, gliosis increased in RML-inoculated mice at 42 dpi and continued until 117 dpi, when the mice developed clinical signs. PrP^{Sc} deposits were detected beginning at 42 dpi (*Middle*), and vacuolation was not evident until late in the disease process (*Bottom*). (Scale bar, 150 μm.)

as determined by the onset of neurological signs and by the point of inflection in BL (Fig. 4*C*).

Discussion

The studies reported here indicate that the point of inflection in BL can serve as a surrogate marker for prion replication. The inverse relationship between prion dose in the inoculum and the BL point of inflection was maintained over the entire range of dilutions investigated (Fig. 4*B*). The accumulation of PrP^{Sc} in prion-infected Tg(*Gfap*-luc) mice, which we detected as early as 42 dpi, preceded increases in GFAP mRNA and BL that were detected at 55 dpi (Figs. 2 and 3). Our findings are consistent with the temporal progression of prion infection reported previously (22).

It will be important to cross the Tg(*Gfap*-luc) mice with various mice, constructed by us and others, that express WT, chimeric, and mutant PrP transgenes. In a preliminary study, we found that bigenic (*Gfap*-luc:MoPrP-A) mice, which overexpress WT mouse PrP-A at ≈8-fold levels of FVB mice, exhibited a BL point of inflection at ≈45 dpi. Based on signs of neurological dysfunction, these Tg(*Gfap*-luc:MoPrP-A) mice had a median incubation time of 52 dpi. Whether higher levels of luc expression will be able to detect gliosis earlier in such mice remains to be determined.

Determining the earliest sites of *Gfap* expression in prion-infected mice will be important in attempting to optimize the bioassay of prions using BLI. In a preliminary study, the trauma of i.c. inoculation was found to incite transient astrocytic gliosis. It may be possible to reduce this gliotic response by using a smaller bore needle and possibly by administering some antiinflammatory drug at the time of or before inoculation. Intraperitoneal inoculation is unfortunately not a useful approach, because it greatly prolongs the incubation time as measured either by the onset of neurological dysfunction or by BLI (Fig. S1) (27, 28).

Defining the pathway from prion multiplication to *Gfap* up-regulation will be paramount to optimizing BLI. GFAP is an intermediate filament protein and, as such, is a member of a large multigene family of highly regulated, abundant cytoskeleton proteins. Astrocyte precursors in the CNS usually express vimentin as the major intermediate filament protein, but during maturation, vimentin expression is down-regulated and GFAP expression increases (29, 30). GFAP is generally recognized as an astrocyte maturation marker. In the mature CNS, *Gfap* expression is regulated dynamically by signals originating from astrocyte-neuronal interactions, as well as neuroendocrine and inflammatory modulators including steroids, cytokines, and growth factors (31, 32).

Changes in gene expression induced by prions were followed throughout the incubation time by measuring mRNA transcripts in murine brains (23). Analysis of a large dataset (≈20 million data points) revealed ≈300 differentially expressed genes (DEGs). Among the highest DEGs during scrapie infection was *Gfap*, as well as some microglial specific genes. Of particular interest, the expression levels for IFN-γ, leukemia inhibitory factor (LIF), IL-2, IL-6, TNF-α, basic fibroblast growth factor (bFGF), IL-1α, and IL-1β, all of which are known to up-regulate *Gfap* expression, did not change throughout the course of the incubation time (23). In RML-infected FVB mice, induction of GFAP was observed between 56–70 dpi, and was closely followed by up-regulation of ciliary neurotrophic factor (CNTF), colony stimulating factor (CSF)-1, and TGF-β1. An earlier study showed up-regulation of the cytokine TGF-β1 after infection, but not of IL-1β, TNF-α, IL-6, or IL-10 (33). In contrast to these foregoing results, several studies reported up-regulation of IL-1β, TNF-α, or IL-6 in the late stage of experimental prion disease (34–38).

BLI has been used to study a mutant SOD Tg model of amyotrophic lateral sclerosis (25). BL increased in the lumbar spinal cord and peripheral nerves of Tg(SOD1,G93A) mice at 4–5 weeks of age when the mice were still asymptomatic. The onset of hind-limb paralysis at 16 weeks of age was also associated with an additional increase in BL, but this increase was

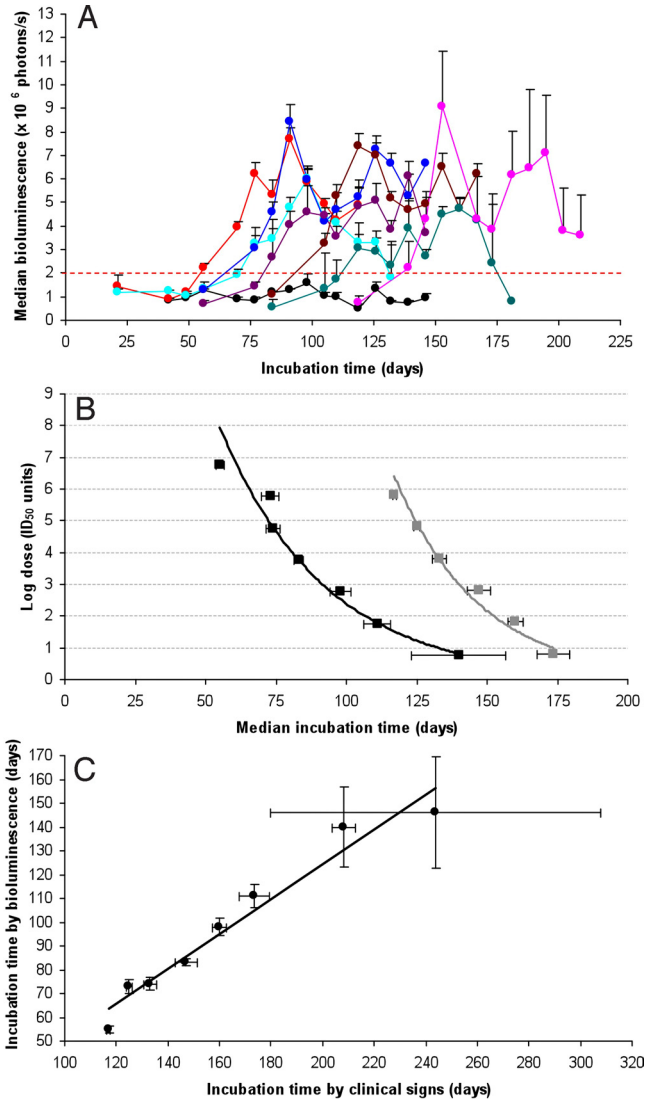

Fig. 4. The inoculated prion dose is related to BL in Tg(*Gfap*-luc) mice. (*A*) Median BL measured from the brains of Tg(*Gfap*-luc) mice inoculated with 10% RML brain homogenate at the following serial log dilutions: −1 (red), −2 (turquoise), −3 (blue), −4 (violet), −5 (brown), −6 (green), and −7 (pink). BL from Tg(*Gfap*-luc) mice inoculated with 1% NBH is shown as a control (black). (*B*) Using the method of Spearman–Kärber, log doses were calculated for the log dilutions shown in *A*, based on the median incubation times for astrocytic gliosis (BL exceeding 2×10^6 photons/s; black curve) and median incubation times for clinical signs (gray curve). BLI detects prion infection from −1 log dilution higher than the incubation-time assay. (*C*) For each dilution, median incubation times for clinical signs plotted against the median incubation times for astrocytic gliosis show a linear relationship. Error bars indicate the SE.

confined to the lumbar region of the spinal cord. BLI has also been used in Tg(*Gfap*-luc) mice to study kainic acid lesions, autoimmune encephalomyelitis, ischemic injury, and pneumococcal meningitis (39–42).

Because *Gfap* expression is so responsive to perturbations in the CNS, BLI of mice expressing the *Gfap*-luc transgene is likely to find wide application in the study of mouse models exhibiting features of neurodegenerative diseases including Parkinson's diseases (PD). Reactive astrocytic gliosis is a prominent attribute of PD (43). Because mouse models of PD lack well defined endpoints and rely on complex behavioral assessments of memory or motor function deficits, mice that express the *Gfap*-luc transgene might offer more readily measurable endpoints of such disease models. If consistent, readily detectable changes can be quantified by BLI, then such an approach may find wide application in studies of the pathogenesis of these and other neurodegenerative diseases.

BLI offers the ability to interrogate repeatedly cellular functions within the brain throughout the prion incubation time, during much of which the mice remain asymptomatic. Our results demonstrated that up-regulation of the *Gfap* gene occurred long before neurological dysfunction developed in Tg(*Gfap*-luc) mice inoculated with prions. Interestingly, the expression of luc remained elevated up to the time of death. BLI of neurodegeneration-induced gliosis not only provides a surrogate marker that is detectable in asymptomatic mice propagating prions, but it also provides an objective measure of prion infection. Most important, BLI permits the quantitative measurement of prion infectivity, because the time interval from inoculation to the BL point of inflection is inversely proportional to the dose of prions inoculated i.c. Because BLI is more rapid, sensitive, and objective than measuring the onset of neurologic dysfunction, it may become the method of choice for studies in which prion infectivity is measured.

Methods

Source of Mice and Husbandry. Tg FVB/N-Tg(*Gfap*-luc)-Xen mice, or Tg(*Gfap*-luc) mice for simplicity, are hemizygous and were provided by Caliper Life Sciences and have been described previously (42). Tg(*Gfap*-luc) mice were maintained by breeding with FVB/N mice. The presence of the *Gfap*-luc transgene in offspring was determined by PCR. The 1-kb PCR product from the sequence internal to the luc gene was amplified using the sense and antisense primer pair 5′-TGGATTCTAAAACGGATTACCAGGG-3′ and 5′-CCAAAACAACAACGGCGGC-3′, both at 0.4 μM in the reaction mix. PCR conditions were 97 °C for 5 min, followed by 35 cycles of 94.5 °C for 40 s, 58 °C for 90 s, and 72 °C for 90 s, followed by a final cycle of 72 °C for 10 min.

Prion Isolates and Transmission. CD1 mouse-adapted RML prions were used as inocula; the RML prion strain was originally derived from sheep with scrapie and has been serially passaged in mice for many generations (44). Brain homogenates (10% wt/vol) in PBS (pH 7.4) were obtained by three 30-s strokes of a PowerGen homogenizer (Fisher Scientific). Serial log dilutions ranging from −1 to −10 for inoculation were obtained by further diluting brain homogenates in 5% (wt/vol) bovine albumin Fraction V (ICN) and PBS. For i.c. inoculation, weanling mice were injected into the right parietal lobe with 30 μL of inoculum using a 27-gauge, disposable hypodermic syringe. For oral inoculation, weanling mice were inoculated by oral gavage using 200 μL of a 1% (wt/vol) brain homogenate. For i.p. inoculations, mice were injected with 200 μL of a 1% (wt/vol) brain homogenate. Inoculated animals were examined daily for their clinical status and three times weekly for neurologic dysfunction, and scored for prion disease based on standard diagnostic criteria (45, 46). All mouse studies were reviewed and approved by the University of California, San Francisco (UCSF) Institutional Animal Care and Use Committee.

BLI. Mice were imaged weekly using an IVIS Spectrum imaging system (Caliper). In brief, mice were injected i.p. with a solution of D-luciferin potassium salt (Caliper) in PBS, pH 7.4 (Invitrogen), receiving 150 mg D-luciferin per kilogram body weight. The mice were then anesthetized using an isofluraneoxygen gas mix and imaged after 10 min for 30–60 s under anesthesia. BL was quantified from images using Living Image 3.0 software (Caliper).

Western Blotting. For Western immunoblotting analysis, 10% (wt/vol) brain homogenates were prepared in PBS containing 2% (wt/vol) N-lauroylsarcosine sodium salt (Sigma-Aldrich) by three runs of 15 s in a Precellys 24 homogenizer (MO Bio Laboratories). Samples of 5% brain homogenates were incubated with 20 μg/mL of proteinase K (PK; New England Biolabs) for 1 h at 37 °C. PK digestion was stopped with 1 mM phenylmethylsulfonyl fluoride (Sigma-Aldrich), and samples were centrifuged at 100,000 × *g* for 1 h at 4 °C. Pellets were resuspended in 90 μL of PBS containing 2% (wt/vol) N-lauroylsarcosine sodium salt before 30 μL of 4× NuPage LDS sample buffer (Invitrogen) was added and the samples were boiled for 5 min. For electrophoresis, 35 μL of undigested and PK-digested samples were loaded onto the gels. SDS gel electrophoresis and Western blotting were performed using Nupage Novex 4–12% Bis-Tris gels and the iBlot dry blotting system (Invitrogen). PrP was detected with the human-mouse (HuM) recombinant antibody fragment

(recFab) P covalently bound to HRP and developed with the enhanced chemiluminescent detection system (Amersham Biosciences) (47).

Quantitative RT-PCR. Brains from euthanized mice were extracted and stored in RNAlater solution (Ambion) at 4 °C overnight and then transferred to −80 °C for long-term storage. In short, brains were taken up in 10 volumes of TRI reagent and homogenized using three runs of 15 s in a Precellys 24 homogenizer (MO Bio Laboratories). Total RNA was extracted using the RiboPure kit (Ambion). Residual DNA was eliminated by DNase treatment using the Turbo DNA-free kit (Ambion). RNA yield was measured using a NanoDrop 1000A spectrophotometer (Thermo Scientific). RNA quality was determined using an Agilent 2100 Bioanalyzer (Agilent Technologies) at the UCSF Helen Diller Family Comprehensive Cancer Center Genome Analysis Core facility. Complementary DNA was made using the SuperScript III Platinum Two-Step qRT-PCR kit with SYBR green (Invitrogen). Real-time PCRs were run on a 7900HT Fast Real-Time PCR System (Applied Biosystems) at the UCSF Genomics Core Facility using the following sense and antisense primer sets: GFAP: 5′-CCGTTCTCTGGAAGACACTGAAAC-3 and 5′-TTGGAAGG ATGGTTGT-GGATTC-3′; 18S: 5′-TTGACGGAAGGGCACCACCAG-3′ and 5′-GCACCACCAC-CCACGGAATCG-3′. Changes in gene expression levels were determined relative to 18S-rRNA, a reference that did not change significantly in our samples.

Histopathology. Tissue samples were either immediately frozen after removal or immersion-fixed in 10% buffered formalin and embedded in paraffin. To evaluate vacuolation, 8-μm-thick brain sections were stained with hematoxylin and eosin (H&E). Reactive astrocytic gliosis was evaluated by immunostaining for GFAP using polyclonal rabbit antiserum Z0334 (Dako). Detection of PrP^{Sc} from formalin-fixed tissue sections was performed with the HuM-P mouse PrP-specific monoclonal antibody after hydrolytic autoclaving, as previously described (48).

ACKNOWLEDGMENTS. We thank Stephen Smith for training on the IVIS Spectrum imaging system, Pierre Lessard and the staff of the Hunters Point animal facility for support with the Tg animal experiments, Ana Serban (University of California, San Francisco, CA) for antibodies, and Hang Nguyen for editorial assistance. This work was supported by a Larry L. Hillblom Foundation fellowship (to G.T.); National Institutes of Health Grants AG02132, AG023501, and AG10770; and the Michael Homer Foundation.

1. Chesebro B (2003) Introduction to the transmissible spongiform encephalopathies or prion diseases. *Br Med Bull* 66:1–20.
2. Weissmann C (2004) The state of the prion. *Nat Rev Microbiol* 2:861–871.
3. Caughey B, Baron GS (2006) Prions and their partners in crime. *Nature* 443:803–810.
4. Prusiner SB (2007) Prions. *Fields Virology*, eds Knipe DM, et al. (Lippincott Williams & Wilkins, Philadelphia), 5th Ed, pp 3059–3092.
5. Aguzzi A, Sigurdson C, Heikenwaelder M (2008) Molecular mechanisms of prion pathogenesis. *Annu Rev Pathol* 3:11–40.
6. Bolton DC, McKinley MP, Prusiner SB (1982) Identification of a protein that purifies with the scrapie prion. *Science* 218:1309–1311.
7. Bendheim PE, Barry RA, DeArmond SJ, Stites DP, Prusiner SB (1984) Antibodies to a scrapie prion protein. *Nature* 310:418–421.
8. Diringer H, Rahn HC, Bade L (1984) Antibodies to protein of scrapie-associated fibrils. *Lancet* 324:345.
9. Chandler RL (1962) Encephalopathy in mice. *Lancet* 279:107–108.
10. Prusiner SB, et al. (1982) Measurement of the scrapie agent using an incubation time interval assay. *Ann Neurol* 11:353–358.
11. Taraboulos A, et al. (1992) Regional mapping of prion proteins in brains. *Proc Natl Acad Sci USA* 89:7620–7624.
12. Prusiner SB, et al. (1980) Molecular properties, partial purification, and assay by incubation period measurements of the hamster scrapie agent. *Biochemistry* 21:4883–4891.
13. Prusiner SB (1982) Novel proteinaceous infectious particles cause scrapie. *Science* 216:136–144.
14. Scott M, et al. (1989) Transgenic mice expressing hamster prion protein produce species-specific scrapie infectivity and amyloid plaques. *Cell* 59:847–857.
15. Carlson GA, et al. (1994) Prion isolate specified allotypic interactions between the cellular and scrapie prion proteins in congenic and transgenic mice. *Proc Natl Acad Sci USA* 91:5690–5694.
16. Flechsig E, Manson JC, Barron R, Aguzzi A, Weissmann C (2004) Knockouts, knockins, transgenics, and transplants in prion research. *Prion Biology and Diseases*, ed Prusiner SB (Cold Spring Harbor Lab Press, Plainview, NY), 2nd Ed, pp 373–434.
17. Bosque PJ, Prusiner SB (2000) Cultured cell sublines highly susceptible to prion infection. *J Virol* 74:4377–4386.
18. Klohn PC, Stoltze L, Flechsig E, Enari M, Weissmann C (2003) A quantitative, highly sensitive cell-based infectivity assay for mouse scrapie prions. *Proc Natl Acad Sci USA* 100:11666–11671.
19. Nishida N, et al. (2000) Successful transmission of three mouse-adapted scrapie strains to murine neuroblastoma cell lines overexpressing wild-type mouse prion protein. *J Virol* 74:320–325.
20. Field EJ (1967) The significance of astroglial hypertrophy in scrapie, kuru, multiple sclerosis and old age together with a note on the possible nature of the scrapie agent. *Dtsch Z Nervenheilkd* 192:265–274.
21. Manuelidis L, Tesin DM, Sklaviadis T, Manuelidis EE (1987) Astrocyte gene expression in Creutzfeldt-Jakob disease. *Proc Natl Acad Sci USA* 84:5937–5941.
22. Jendroska K, et al. (1991) Proteinase-resistant prion protein accumulation in Syrian hamster brain correlates with regional pathology and scrapie infectivity. *Neurology* 41:1482–1490.
23. Hwang D, et al. (2009) A systems approach to prion disease. *Mol Syst Biol* 5:252.
24. Tatzelt J, et al. (1996) Scrapie in mice deficient in apolipoprotein E or glial fibrillary acidic protein. *Neurology* 47:449–453.
25. Keller AF, Gravel M, Kriz J (2009) Live imaging of amyotrophic lateral sclerosis pathogenesis: Disease onset is characterized by marked induction of GFAP in Schwann cells. *Glia 57:1130–1142.*
26. Dougherty R (1964) Animal virus titration techniques. *Techniques in Experimental Virology*, ed Harris RJC (Academic, New York), pp 169–224.
27. Kimberlin RH, Walker CA (1982) Pathogenesis of mouse scrapie: Patterns of agent replication in different parts of the CNS following intraperitoneal infection. *J R Soc Med* 75:618–624.
28. Kimberlin RH, Walker CA (1986) Pathogenesis of scrapie (strain 263K) in hamsters infected intracerebrally, intraperitoneally or intraocularly. *J Gen Virol* 67:255–263.
29. Pixley SK, de Vellis J (1984) Transition between immature radial glia and mature astrocytes studied with a monoclonal antibody to vimentin. *Dev Brain Res* 317:201–209.
30. Wofchuk ST, Rodnight R (1995) Age-dependent changes in the regulation by external calcium ions of the phosphorylation of glial fibrillary acidic protein in slices of rat hippocampus. *Dev Brain Res* 85:181–186.
31. Laping NJ, Teter B, Nichols NR, Rozovsky I, Finch CE (1994) Glial fibrillary acidic protein: Regulation by hormones, cytokines, and growth factors. *Brain Pathol* 4:259–275.
32. Gomes FC, Paulin D, Moura Neto V (1999) Glial fibrillary acidic protein (GFAP): Modulation by growth factors and its implication in astrocyte differentiation. *Braz J Med Biol Res* 32:619–631.
33. Cunningham C, Boche D, Perry VH (2002) Transforming growth factor beta1, the dominant cytokine in murine prion disease: Influence on inflammatory cytokine synthesis and alteration of vascular extracellular matrix. *Neuropathol Appl Neurobiol* 28:107–119.
34. Williams A, Van Dam AM, Ritchie D, Eikelenboom P, Fraser H (1997) Immunocytochemical appearance of cytokines, prostaglandin E2 and lipocortin-1 in the CNS during the incubation period of murine scrapie correlates with progressive PrP accumulations. *Brain Res* 754:171–180.
35. Campbell IL, Eddleston M, Kemper P, Oldstone MB, Hobbs MV (1994) Activation of cerebral cytokine gene expression and its correlation with onset of reactive astrocyte and acute-phase response gene expression in scrapie. *J Virol* 68:2383–2387.
36. Kordek R, et al. (1996) Heightened expression of tumor necrosis factor alpha, interleukin 1 alpha, and glial fibrillary acidic protein in experimental Creutzfeldt-Jakob disease in mice. *Proc Natl Acad Sci USA* 93:9754–9758.
37. Schultz J, et al. (2004) Role of interleukin-1 in prion disease-associated astrocyte activation. *Am J Pathol* 165:671–678.
38. Van Everbroeck B, et al. (2002) The role of cytokines, astrocytes, microglia and apoptosis in Creutzfeldt-Jakob disease. *Neurobiol Aging* 23:59–64.
39. Cordeau P, Jr, Lalancette-Hebert M, Weng YC, Kriz J (2008) Live imaging of neuroinflammation reveals sex and estrogen effects on astrocyte response to ischemic injury. *Stroke* 39:935–942.
40. Kadurugamuwa JL, et al. (2005) Reduction of astrogliosis by early treatment of pneumococcal meningitis measured by simultaneous imaging, in vivo, of the pathogen and host response. *Infect Immun* 73:7836–7843.
41. Luo J, Ho P, Steinman L, Wyss-Coray T (2008) Bioluminescence in vivo imaging of autoimmune encephalomyelitis predicts disease. *J Neuroinflammation* 5:6.
42. Zhu L, et al. (2004) Non-invasive imaging of GFAP expression after neuronal damage in mice. *Neurosci Lett* 367:210–212.
43. McGeer PL, McGeer EG (2008) Glial reactions in Parkinson's disease. *Mov Disord* 23:474–483.
44. Chandler RL (1961) Encephalopathy in mice produced by inoculation with scrapie brain material. *Lancet* 277:1378–1379.
45. Carlson GA, et al. (1988) Genetics and polymorphism of the mouse prion gene complex: Control of scrapie incubation time. *Mol Cell Biol* 8:5528–5540.
46. Scott M, et al. (1993) Propagation of prions with artificial properties in transgenic mice expressing chimeric PrP genes. *Cell* 73:979–988.
47. Tamgüney G, et al. (2008) Genes contributing to prion pathogenesis. *J Gen Virol* 89:1777–1788.
48. Muramoto T, et al. (1997) Heritable disorder resembling neuronal storage disease in mice expressing prion protein with deletion of an α-helix. *Nat Med* 3:750–755.